

# Sustainable Food Technology

Accepted Manuscript

This article can be cited before page numbers have been issued, to do this please use: S. R. P. Putri, D. Haryati, U. Santoso, A. Ningrum, A. Nugrahini and -. Manikharda, *Sustainable Food Technol.*, 2025, DOI: 10.1039/D5FB00316D.



This is an Accepted Manuscript, which has been through the Royal Society of Chemistry peer review process and has been accepted for publication.

Accepted Manuscripts are published online shortly after acceptance, before technical editing, formatting and proof reading. Using this free service, authors can make their results available to the community, in citable form, before we publish the edited article. We will replace this Accepted Manuscript with the edited and formatted Advance Article as soon as it is available.

You can find more information about Accepted Manuscripts in the [Information for Authors](#).

Please note that technical editing may introduce minor changes to the text and/or graphics, which may alter content. The journal's standard [Terms & Conditions](#) and the [Ethical guidelines](#) still apply. In no event shall the Royal Society of Chemistry be held responsible for any errors or omissions in this Accepted Manuscript or any consequences arising from the use of any information it contains.

Sustainability Spotlight Statement

View Article Online  
DOI: 10.1039/D5FB00316D

This study addresses sustainability by transforming underutilized rabbit bone waste into biodegradable edible films, offering a value-added alternative to petroleum-based plastic packaging. Rabbit bone gelatin provides a culturally acceptable and halal-compatible substitute for bovine and porcine gelatin, with superior gel-forming ability compared to fish-derived gelatin. The development of these films supports SDG 12 (Responsible Consumption and Production) by reducing plastic use and promoting circular economy principles through animal by-product valorization. Glycerol concentration was optimized to balance film flexibility and barrier properties. Application testing using soybean oil demonstrated the film's protective function. Overall, this research advances sustainable packaging innovation by integrating waste utilization, material functionality, and food quality preservation.



## ARTICLE

## Rabbit Bone Gelatin Edible Films: Impact of Glycerol Concentration on Properties and Application in Soybean Oil Packaging

Siti Rima Pratiwi Putri,<sup>a</sup> Dian Haryati,<sup>a</sup> Umar Santoso,<sup>a</sup> Andriati Ningrum,<sup>a</sup> and Ashri Nugrahini<sup>a</sup> and Manikharda<sup>\*a</sup>

Received 00th January 20xx,  
Accepted 00th January 20xx

DOI: 10.1039/x0xx00000x

Rabbit bone, a by-product of rabbit meat processing, remains underutilized and is often discarded as waste. However, its high collagen content makes it a promising alternative source of gelatin for developing biodegradable edible films as replacements for plastic packaging. This study investigated the effect of varying glycerol concentrations (RG20:20%, RG30:30%, and RG40:40%) on the physicochemical, mechanical, barrier, optical, and thermal properties of rabbit bone gelatin-based films, and evaluated their potential application in soybean oil packaging. A bovine gelatin film with 30% glycerol served as control. Increasing glycerol concentrations led to higher moisture content (9.96–19.16%), thickness (0.087–0.109 mm), solubility (31.77–50.84%), water vapor permeability (WVP) ( $0.63$  to  $2.43 \times 10^{-9}$  g·m<sup>-1</sup>·Pa<sup>-1</sup>·s<sup>-1</sup>), and elongation at break (99.29–163.11%). However, reduced opacity value (2.13 to 1.62), tensile strength (7.34 to 3.00), and melting temperature (178.46 to 149.34 °C). Among the formulations, RG20 film exhibited superior tensile strength, barrier, thermal, and optical properties, confirming the functional promise of rabbit bone gelatin for edible film development. RG20 film was selected for further testing, compared with LDPE packaging. On day 9, the peroxide value of soybean oil exhibited a more rapid increase in LDPE (13.12 meq O<sub>2</sub>/kg) than RG20 (6.57 meq O<sub>2</sub>/kg). However, RG20 film was less effective in inhibiting the increase of anisidine value (12.15) compared to LDPE (6.5) on early storage period. Free fatty acid levels remained relatively stable in both treatments, indicating minimal hydrolytic degradation. These findings suggest that RG films have potential use as a biodegradable alternative for soybean oil packaging.

### 1 Introduction

Rabbit bones remain an underutilized by-product of rabbit meat processing, mostly treated as slaughterhouse waste, despite their potential to be processed into value-added products, such as gelatin. Gelatin is a hydrocolloid protein derived from the partial hydrolysis of collagen, one of the main components of bone, accounting for approximately 25% of the total components.<sup>1</sup> The utilization of rabbit bone-derived gelatin adds economic value and supports Sustainable Development Goals (SDGs) 12 on responsible consumption and production. Commercial gelatin is primarily sourced from bovine and porcine materials, posing religious and cultural challenges. Therefore, rabbit bone gelatin represents a promising alternative that is more widely acceptable across different consumer groups. Fish-derived gelatin has been explored as an alternative; however, fish gelatin has a lower gel-forming ability than mammalian gelatin due to its lower hydroxyproline and proline content, two amino acids that affect the stability of gelatin molecule conformation.<sup>2</sup> Therefore, alternative mammalian sources with desirable gel-forming

characteristics and fewer cultural concerns, such as rabbit bones, warrant further investigation.

One potential application of gelatin is as a raw material for producing edible films, which can serve as biodegradable food packaging. Currently, the food packaging sector remains dominated by conventional petroleum-based plastics, which are non-biodegradable and contribute to environmental pollution.<sup>3</sup> As the demand for packaged foods continues to grow, plastic waste is also increasing. Gelatin-based edible films offered an eco-friendly alternative to conventional plastic packaging. Based on preliminary findings that rabbit bone gelatin exhibits comparable gel-forming abilities to commercial bovine gelatin due to its amino acid composition, this study seeks to empirically test its effectiveness in film formation and its protective qualities in food packaging, thereby providing a scientific basis for its potential as a sustainable packaging solution.

A critical factor in developing edible films is using plasticizers, such as glycerol, which improve elasticity, flexibility, and prevent brittleness by interacting with polar peptide chains in gelatin matrix.<sup>4</sup> Consistent with the present results, Rosmawati *et al.*<sup>5</sup> reported that glycerol yielded more flexible films than sorbitol. The concentration of glycerol plays a significant role in determining film characteristics. Studies by Ozcan *et al.*<sup>6</sup> and Lau and Sarbon<sup>7</sup> reported that higher glycerol levels increased film elasticity, while tensile strength decreased

<sup>a</sup> Department of Food and Agricultural Product Technology, Faculty of Agricultural Technology, Gadjah Mada University, Jalan Flora No 1, Bulaksumur, Sleman, 55281 Yogyakarta, Indonesia.

<sup>†</sup> Electronic supplementary information (ESI) available. See DOI: 10.1039/x0xx00000x



due to hydrogen bonds between glycerol hydroxyl groups and gelatin polymer matrix. These interactions resulted in more cohesive and compact structure. However, due to the hygroscopic nature of glycerol, excessive glycerol in film formulation can increase moisture content and accelerate oxidative degradation of packaged products.<sup>8</sup> On the other hand, insufficient glycerol concentration may result in strong but brittle films due to limited polymer chain mobility.<sup>7</sup> Therefore, optimizing glycerol concentration was crucial to obtaining edible films with desirable mechanical and barrier characteristics.

Nevertheless, gelatin-based edible films are inherently hydrophilic, which limits their application in high-moisture food products but makes them suitable for packaging hydrophobic materials such as oils.<sup>8</sup> This study selected soybean oil as the model product due to its high polyunsaturated fatty acids content, making it highly susceptible to oxidation. This clearly evaluates the film's ability to protect against oxidative deterioration. Moreover, soybean oil is widely used as a cooking oil in household and industrial applications, making it a relevant model for evaluating the protective functionality of rabbit bone gelatin films in edible oil packaging systems.

While the physicochemical properties of rabbit bone gelatin have been examined in prior studies,<sup>9</sup> the development and comprehensive characterization of edible films based on this gelatin have not been previously reported. Therefore, this study was designed to examine how varying glycerol concentrations influence the physicochemical, mechanical, barrier, optical, and thermal properties of rabbit bone gelatin films, as well as their performance as oil packaging compared with conventional LDPE plastics. We hypothesized that increasing glycerol concentration would significantly alter film characteristics and that the best-performing concentration would yield a rabbit bone gelatin film with balanced strength, flexibility, and barrier properties. Such a formulation is expected to serve as a viable and sustainable alternative to petroleum-based packaging, particularly for oxidative-sensitive products such as soybean oil. The objectives of this study were to develop and characterize edible films from rabbit bone gelatin with different glycerol concentrations, compare them with commercial bovine gelatin films, and evaluate their potential as biodegradable packaging for soybean oil under storage conditions.

## 2 Materials and methods

### 2.1 Materials

Rabbit bones, specifically rib bones from New Zealand and Rex breeds aged 4–6 months, were obtained from Magetan, East Java, Indonesia. The fresh rabbit bones were immediately boiled for 1 h, cleaned, cut into 1–2 cm in size, and stored in a freezer at -18 °C prior to extraction. Commercial bovine gelatin (Hays Food & Co, Indonesia), soybean oil (Mazola, MOI FOODS, Malaysia), low-density polyethylene (LDPE) plastic, and glycerol were purchased from a local market.

### 2.2 Rabbit bone gelatine extraction

Gelatin from rabbit bones was extracted according to Wulandari *et al.*<sup>9</sup> with modifications. The bones were soaked in 6% HCl solution (1:3 w/v) for 4 days at 30 °C, with the solution replaced every 2 days, to obtain ossein. After immersion, ossein was washed with flowing water, and then soaked in 0.25 M EDTA (1:2 w/v) for 2 days. Before extraction, ossein was washed with flowing water until neutral pH. Extraction was performed in a water bath (Memmert WNB 29, Schwabach, Germany) at gradient temperatures (65 °C, 75 °C, and 85 °C), each for 4 h, using 1:2 (w/v) ossein-to-distilled water ratio, with distilled water replaced at each step. The extract was filtered, dried at 50 °C for 16 h, and milled into powder.

### 2.3 Preparation of Films

Films were prepared following the method of Theerawitayaart *et al.*<sup>10</sup> with modifications. Gelatin solution (8% w/w) was prepared by dissolving rabbit bone gelatin or bovine gelatin in 15 mL of distilled water and heated at 60 °C for 30 min. Glycerol was added as a plasticizer at concentrations of 20%, 30%, and 40%, based on the gelatin weight, then stirred for 5 min. For bovine gelatin (BG) film, 30% glycerol was used. These films were labeled as RG20, RG30, RG40, and BG30. The film-forming solution was poured into rectangular molds (130 × 85 mm) and dried in a food dehydrator (FDH-8 Wirastar, Semarang, Indonesia) at 50 °C for 10 h. The dried films were stored in a desiccator containing Mg(NO<sub>3</sub>)<sub>2</sub> (53% Relative Humidity, RH) at 27 ± 1 °C for at least 12 h before being manually removed from the molds and analyzed.

### 2.4 Physicochemical properties of films

#### 2.4.1 Thickness

The thickness of the edible film was measured using a digital micrometer (Mitutoyo Series 293, Kawasaki, Japan) with an accuracy of 0.001 mm. Measurements were taken randomly at different points, and the average film thickness was then calculated.

#### 2.4.2 Moisture content (MC)

MC analysis was performed following the AOAC<sup>11</sup> method. The film sample was weighed ( $w_0$ ) and dried in an oven (Memmert UN110, Schwabach, Germany) at 100–105 °C until a constant weight was achieved ( $w_1$ ). The final weight was recorded, and MC was calculated using Eq. 1:

$$MC (\%) = \frac{w_0 - w_1}{w_0} \times 100 \quad (1)$$

#### 2.4.3 Water solubility (WS)

According to Wang *et al.*,<sup>12</sup> films (20 × 20 mm) were dried in an oven (Memmert UN110) at 105 °C until a constant weight was achieved. The initial dry weight ( $m_0$ ) was recorded. The film was then immersed in 10 mL of distilled water at 27 ± 1 °C for 24 hours. The solution was filtered using pre-dried filter paper, and the remaining film residue was dried in an oven (Memmert UN110) at 105 °C. The final dry weight ( $m_1$ ) was recorded. The WS was calculated using Eq. 2:

View Article Online

DOI: 10.1039/D5FO00316D



$$WS(\%) = \frac{m_0 \times m_1}{m_0} \times 100 \quad (2)$$

## 2.5 Water vapor permeability (WVP)

WVP was analyzed based on the method of ASTM-E96/E96M.<sup>13</sup> Films (40 × 40 mm) were measured for thickness and placed over the mouth of 5 mL glass bottles (d = 1 cm) containing 5.5 g CaCl<sub>2</sub> (0% RH), ensuring an airtight seal. The initial weight was recorded, and the bottle was placed in a desiccator at 27 ± 1 °C and 50 ± 1% RH for 8 h, with weight recorded hourly. WVP was calculated using using Eq. 3:

$$WVP = \frac{m \times L}{t \times A \times S (R1 - R2)} \quad (3)$$

where *m* was absorbed water vapor (g); *L* was film thickness (mm); *t* was test duration (s); *A* is effective film area (m<sup>2</sup>); *S* was saturated water vapor pressure at 27 °C (3565 Pa); *R1* and *R2* were RH in the test chamber (50%) and inside the bottle (0%)

## 2.6 Tensile strength (TS) and elongation at break (EAB)

The mechanical properties of the edible film, including TS and EAB, were determined as described by Leite *et al.*<sup>14</sup> using a Universal Testing Machine (ZwickRoell Z0.5, Ulm, Germany) equipped with a 100 N load cell. Film samples (100 × 50 mm) were elongated at a crosshead speed of 10 mm/min with an initial grip separation of 50 mm.

## 2.7 Optical properties of films

Color intensity was measured using a chroma meter (Konica Minolta CR-400, America) based on the CIELAB system, which evaluates L\*, a\*, and b\* values. Transmittance and opacity were analyzed following the method of Hajlaoui *et al.*<sup>15</sup> The film was placed directly into a cuvette, and transmittance was measured using a UV-Vis spectrophotometer (Shimadzu UV-1280, Kyoto, Japan). Light transmittance was recorded at UV and visible wavelengths ranging from 200 to 800 nm at 100 nm intervals. The transmittance value at 600 nm and the film thickness (*x*) were used to calculate film opacity using Eq. 4:

$$\text{Opacity} = \frac{-\log T_{600}}{x} \quad (4)$$

## 2.8 Thermal properties

Thermal properties were analyzed using differential scanning calorimetry following the method described by Zhang *et al.*<sup>16</sup> Edible film samples weighing 3 mg were placed and sealed in aluminum pans. The samples were then scanned over a temperature range of 20–250 °C at a heating rate of 10 °C/min to determine the melting temperature (*T<sub>m</sub>*) of the edible films.

## 2.9 Fourier transform infrared (FTIR) spectroscopy

FTIR analysis was conducted following the method of Hajlaoui *et al.*<sup>15</sup> Circular film samples (d = 5 mm) were analyzed using an attenuated total reflection-fourier transform infrared spectrometer (ATR-FTIR) (Thermo Nicolet Avatar 370 FT-IR, Madison, USA). Each sample was scanned 32 times over the range of 4000 cm<sup>-1</sup> to 650 cm<sup>-1</sup> at a resolution of 4 cm<sup>-1</sup>. A blank background spectrum was recorded before each scan. Spectral data were then processed using Spectrum software, including background subtraction, baseline correction, smoothing, and normalization.

## 2.10 Scanning electron microscopy (SEM)

View Article Online

DOI: 10.1016/j.sft.2025.100716

The surface and cross-sectional microstructure of the films were observed using SEM (JEOL SM-IT700HR, Tokyo, Japan) with SMILEVIEW Lab software. Film samples (2 × 2 mm) were mounted on a copper stub and coated with a thin layer of gold. The samples were then scanned at an acceleration voltage of 10 kV, with magnifications of 5000× for the surface morphology and 500× for the cross-section.

## 2.11 Soybean oil packaging applications

### 2.11.1 Packaging preparation

The RG20 film, which possessed satisfactory mechanical and barrier properties against water vapor and light, was selected to prepare soybean oil pouches (35 × 60 mm). The film was folded and heat-sealed on two sides using a 120–130 °C sealer, filled with 8 mL of soybean oil, and sealed on the remaining side. LDPE packaging was prepared following the method described by Niluwan *et al.*<sup>17</sup> and used as the control. All oil packages were stored in a desiccator at 27 ± 1 °C and 50 ± 1% relative humidity (RH) for 15 days. Oxidative stability was assessed based on peroxide value (PV), anisidine value (AV), and free fatty acid (FFA) content, measured on days 0, 3, 6, 9, 12, and 15 with duplicate analyses for each time point.

### 2.11.2 Peroxide value of soybean oil

PV was determined according to the method of Wang *et al.*<sup>18</sup> Soybean oil (1.5 g) was dissolved in 15 mL of acetic acid:chloroform (2:3, v/v), followed by adding 1 mL of 70% KI. The mixture was kept in the dark for 5 min to allow color development. Then, 15 mL of distilled water and 1 mL of 1% starch indicator were added, and the solution was titrated with 0.1 mol/L Na<sub>2</sub>S<sub>2</sub>O<sub>3</sub> until the color changed from dark brown to milky white. The PV was calculated using Eq. 5:

$$PV (\text{meq O}_2/\text{kg}) = \frac{(V_1 - V_0) \times c \times 1000}{m} \quad (5)$$

where *V<sub>1</sub>* and *V<sub>0</sub>* were the volume of Na<sub>2</sub>S<sub>2</sub>O<sub>3</sub> solution (mL) used for the sample and blank; *c* was Na<sub>2</sub>S<sub>2</sub>O<sub>3</sub> solution concentration (mol/L); and *m* was the weight of the oil sample (g).

### 2.11.3 Anisidine value of soybean oil

AV was determined based on the ISO 6885<sup>19</sup> method. Soybean oil was dissolved in isooctane to a final concentration of 0.05 g/mL. Absorbance was measured at 350 nm using a UV-Vis spectrophotometer (Shimadzu UV-1280), with pure isooctane as the blank. For the reactive test solution, 5 mL of sample solution was mixed with 1 mL of 0.75% anisidine solution and incubated in the dark for 10 min. A blank solution was prepared using 5 mL of isooctane instead of the sample. The non-reactive solution consisted of 5 mL of the sample and 1 mL of glacial acetic acid, also incubated in the dark for 10 min. The AV was calculated using Eq. 6:

$$AV = \frac{100 \times QV}{m} \times [1.2 \times (Abs_1 - Abs_2 - Abs_0)] \quad (6)$$

where *Q* was sample concentration (g/mL); *V* was the volume of total sample (mL); *m* was the weight of the oil sample (g);





$Abs_1$ ,  $Abs_2$ , and  $Abs_0$  were the absorbance of reactive test solution, non-reactive test solution, and blank solution.

2.11.4 Free fatty acid (FFA) of soybean oil

FFA content was analyzed following the ISO 660<sup>20</sup> method. Soybean oil (1 g) was dissolved in 30 mL of ethanol, followed by adding 2 mL of phenolphthalein indicator. The solution was titrated with 0.1 mol/L NaOH until a faint pink color persisted. FFA was calculated using Eq. 7:

$$FFA\text{ (\% oleic acid)} = \frac{VcM \times 100}{1000 \times m} \tag{7}$$

where  $V$  was the volume of NaOH solution (mL);  $c$  was NaOH solution concentration (mol/L);  $M$  was molecular mass of oleic acid (g/mol); and  $m$  was the weight of the oil sample (g).

2.12 Statistical analysis

This research was structured using factorial experiments, and a completely randomized design (CRD) was implemented. Statistical analysis was conducted using SPSS software (Version 20.0, IBM Corp., Armonk, NY, USA). One-way ANOVA followed by Duncan’s test ( $p < 0.05$ ) was used to analyze edible film properties. T-tests and one-way ANOVA were used to compare soybean oil quality across packaging types and storage durations. All data in the tables are expressed as mean  $\pm$  standard deviation (SD).

3 Results and discussion

3.1 Characteristics of films

3.1.1 Thickness

The thickness of gelatin films significantly increased with higher glycerol concentrations, as shown in Table 1. The thickest film was RG40 (0.109 mm), followed by RG30, BG30, and RG20 film. This trend suggests that glycerol, acting as a plasticizer, enhances film thickness by increasing free volume and reducing intermolecular interactions within the polymer matrix. The hygroscopic nature of glycerol also promotes moisture retention, contributing to matrix expansion. Similar results have been reported in rabbit skin gelatin films, where the addition of

glycerol led to increased film thickness.<sup>21</sup> Previous studies have shown that incorporating glycerol into biopolymer films enhances their ductility while reducing intra- and intermolecular forces within the polymer network.<sup>22</sup> Moreover, the increased water content associated with glycerol addition can further expand the polymer structure, reinforcing the trend of increasing thickness.<sup>23</sup>

3.1.2 Moisture Content

Moisture content increased significantly with higher glycerol concentrations, as shown in Table 1. RG20 film had the lowest moisture content (9.96%), significantly lower than BG30 (13.69%), while the highest value was observed in RG40 film at 19.16%. The hygroscopic nature of glycerol, characterized by its three hydroxyl groups (-OH), contributes to increased moisture content of films as glycerol concentration rises. These hydroxyl groups have strong affinity and form hydrogen bonds with water molecules, enhancing water absorption capacity of films.<sup>24</sup> Glycerol also increases the free volume within the polymer matrix, facilitating moisture uptake.<sup>25</sup> This trend aligns with previous studies, which also reported higher moisture content in turkey skin gelatin films with 40% glycerol, namely 22.46%.<sup>6</sup> Additionally, an increase in moisture content was associated with greater film thickness, as the plasticizing effect of glycerol influenced both properties.

3.1.3 Water Solubility

The solubility of gelatin films varied significantly with different glycerol concentrations, as shown in Table 1. The control film (BG30) demonstrated a solubility of 43.91%, while the RG20 film exhibited a lower solubility of 31.77%. This reduction suggested that decreasing glycerol concentration created a more stable film structure with enhanced water resistance, attributed to a denser protein network with fewer hydrophilic groups. An association between moisture content and solubility was observed, where BG30 had a higher moisture content than the RG20 film (Table 1). This indicated that films with higher moisture retention were more susceptible to dissolution. As a plasticizer, glycerol influenced the structure and properties of the films.<sup>26</sup>

**Table 1.** Thickness, moisture content, water solubility, water vapor permeability, tensile strength, elongation at break, color, and opacity of edible films with different glycerol concentrations

Parameters	BG30	RG20	RG30	RG40
Thickness (mm)	0.094 $\pm$ 0.006 <sup>b</sup>	0.087 $\pm$ 0.003 <sup>a</sup>	0.101 $\pm$ 0.005 <sup>c</sup>	0.109 $\pm$ 0.004 <sup>d</sup>
Moisture content (%)	13.69 $\pm$ 1.35 <sup>b</sup>	9.96 $\pm$ 0.44 <sup>a</sup>	14.47 $\pm$ 0.81 <sup>b</sup>	19.16 $\pm$ 1.29 <sup>c</sup>
Water Solubility (%)	43.91 $\pm$ 2.85 <sup>b</sup>	31.77 $\pm$ 0.93 <sup>a</sup>	44.70 $\pm$ 4.94 <sup>bc</sup>	50.84 $\pm$ 5.34 <sup>c</sup>
WVP (10 <sup>-9</sup> g·m <sup>-1</sup> ·Pa <sup>-1</sup> ·s <sup>-1</sup> )	1.21 $\pm$ 0.00 <sup>a</sup>	0.632 $\pm$ 0.00 <sup>b</sup>	1.25 $\pm$ 0.00 <sup>a</sup>	2.43 $\pm$ 0.00 <sup>c</sup>
Tensile Strength (MPa)	5.41 $\pm$ 0.63 <sup>c</sup>	7.34 $\pm$ 0.30 <sup>d</sup>	4.24 $\pm$ 0.58 <sup>b</sup>	3.00 $\pm$ 0.27 <sup>a</sup>
EAB (%)	171.34 $\pm$ 10.22 <sup>c</sup>	99.29 $\pm$ 11.36 <sup>a</sup>	133.83 $\pm$ 5.05 <sup>b</sup>	163.11 $\pm$ 9.25 <sup>c</sup>
Color				
$L^*$	41.68 $\pm$ 0.97 <sup>b</sup>	40.04 $\pm$ 2.25 <sup>a</sup>	40.18 $\pm$ 2.21 <sup>ab</sup>	40.22 $\pm$ 1.94 <sup>ab</sup>
$a^*$	-0.10 $\pm$ 0.04 <sup>b</sup>	-0.26 $\pm$ 0.07 <sup>a</sup>	-0.26 $\pm$ 0.07 <sup>a</sup>	-0.27 $\pm$ 0.08 <sup>a</sup>
$b^*$	0.20 $\pm$ 0.08 <sup>a</sup>	1.80 $\pm$ 0.20 <sup>c</sup>	1.71 $\pm$ 0.17 <sup>bc</sup>	1.67 $\pm$ 0.08 <sup>b</sup>
Opacity	0.67 $\pm$ 0.23 <sup>a</sup>	2.13 $\pm$ 0.50 <sup>c</sup>	1.82 $\pm$ 0.44 <sup>bc</sup>	1.62 $\pm$ 0.39 <sup>b</sup>



All data in the tables are expressed as mean  $\pm$  standard deviation (SD). Different lowercase letters in the same row indicate significant difference ( $p < 0.05$ ).  
DOI: 10.1039/D5FB00316D

As the glycerol concentration increased, water solubility rose due to enhanced hydrophilicity and disruption of polymer cohesion.<sup>27</sup> The RG40 film showed the highest solubility (50.84%), supporting the trend and consistent with previous studies on the plasticizing effect of glycerol in duck feet gelatin film.<sup>24</sup>

### 3.1.4 Water Vapor Permeability (WVP)

WVP of gelatin films varied significantly with glycerol concentration (Table 1). RG20 film exhibited the lowest WVP ( $0.632 \times 10^{-9} \text{ g} \cdot \text{m}^{-1} \cdot \text{Pa}^{-1} \cdot \text{s}^{-1}$ ), indicating superior barrier properties, while the highest WVP was observed in RG40 film ( $2.43 \times 10^{-9} \text{ g} \cdot \text{m}^{-1} \cdot \text{Pa}^{-1} \cdot \text{s}^{-1}$ ). The BG30 showed a WVP of  $1.21 \times 10^{-9} \text{ g} \cdot \text{m}^{-1} \cdot \text{Pa}^{-1} \cdot \text{s}^{-1}$ , comparable to the rabbit gelatin film with the same glycerol level. The increased WVP at higher glycerol concentrations is likely due to enhanced hydrophilicity and reduced polymer cohesion, resulting in a looser matrix more permeable to water vapor. These findings are consistent with the solubility and moisture content trends, where higher glycerol levels corresponded to higher water uptake and lower barrier integrity. Similar patterns have been reported in gelatin-based films, where glycerol addition increased WVP due to plasticization effects.<sup>21,24</sup> However, Galus *et al.*<sup>27</sup> observed a WVP reduction in sodium caseinate films when glycerol was combined with hydrophobic waxes, suggesting that other film components can modulate the effect of glycerol. Overall, RG20 film appeared optimal for minimizing WVP, although higher levels may be preferred when prioritizing flexibility over barrier function.

### 3.1.5 Tensile Strength

Glycerol concentration significantly affected the TS of films (Table 1). RG20 film exhibited the highest tensile strength (7.34 MPa), significantly higher than BG30 film (5.41 MPa). However, increasing the glycerol concentration to 30% and 40% resulted in a marked reduction in tensile strength to 4.24 MPa and 3.00 MPa, respectively. This decline was attributed to the plasticizing effect of glycerol, which promoted polymer chain mobility and reduced intermolecular interactions, resulting in increased flexibility but reduced mechanical strength.<sup>25</sup> These results suggested that 20% glycerol was the optimal concentration for maximizing the TS. The great TS of RG films could be attributed to the quality of rabbit bone gelatin obtained through a modified extraction process, where the gel strength reached  $212.81 \pm 4.48 \text{ g Bloom}$  (Table S1). A higher gelatin gel strength was directly correlated with improved mechanical properties of the films, whereby stronger gels contributed to higher TS.<sup>28</sup>

### 3.1.6 Elongation At Break (EAB)

**Table 2.** Light transmittance of edible films with different glycerol concentrations

Films	Wavenumber (nm)					
	200	300	400	500	600	700

EAB of gelatin films showed notable variation with different glycerol concentrations (Table 1). BG30 film had the highest EAB (171.34%) and was similar ( $p > 0.05$ ) to RG40 film (163.11%), while RG20 film exhibited a significantly lower value (99.29%). This indicates that both gelatin source and glycerol level influence film extensibility. Increasing glycerol from 20% to 40% improved EAB, likely due to the plasticizing effect of glycerol, which enhances flexibility and stretchability by increasing free volume and reducing intermolecular forces within the polymer matrix. However, the optimal concentration depends on the polymer system and interactions with other components.<sup>29</sup> This trend has also been observed in gelatin-based films; EAB increased from 71.64% to 193.76% as glycerol levels rose from 10% to 40%.<sup>7</sup>

### 3.1.7 Color and Opacity

The color attributes ( $L^*$ ,  $a^*$ ,  $b^*$ ) and opacity of gelatin films varied with gelatin source and glycerol concentration, as presented in Table 1. BG30 film had the highest lightness ( $L^* = 41.68$ ), slight greenish tint ( $a^* = -0.10$ ), and slight yellow hue ( $b^* = 0.20$ ) alongside the lowest opacity (0.67). In contrast, RG films appeared slightly darker ( $L^* \approx 40$ ), with more negative  $a^*$  values ( $-0.26$  to  $-0.27$ ) and significantly higher  $b^*$  values (1.67–1.80), indicating a more intense yellow coloration. These results were likely due to the differences in gelatin sources, where the amino acids cysteine and methionine contribute to a more yellow color, as well as variations in extraction methods and pH levels used.<sup>21,30</sup> Yellowness was decreased in the films with higher glycerol could be linked to the dilution of proteins since glycerol is a colorless compound.<sup>21</sup> Opacity was notably greater in RG films, peaking at 20% glycerol (2.13), and declined with increasing glycerol levels. The observed optical variations are attributed to the plasticizing effect of glycerol, which enhances film flexibility and homogeneity by disrupting polymer chain regularity. It resulted in a less compact matrix, facilitating greater light transmission and enhanced film transparency.<sup>6</sup>

### 3.1.8 Transmittance

Film transmittance was influenced by both glycerol concentration and gelatin source (Table 2). Films that transmit higher amounts of light could expose the packaged food to photooxidation, reducing its shelf life.<sup>31</sup> In the UV range (200–280 nm), all films exhibited low transmittance values (0.02–0.05%), which gradually increased beyond 280 nm. This behavior indicated that the films might protect against UV-induced oxidation to a certain level.

BG30	0.05 ± 0.01 <sup>d</sup>	53.29 ± 4.62 <sup>d</sup>	80.89 ± 2.80 <sup>d</sup>	86.81 ± 0.96 <sup>d</sup>	87.83 ± 1.81 <sup>e</sup>	88.38 ± 0.75 <sup>d</sup>	89.10 ± 0.56 <sup>d</sup>
RG20	0.02 ± 0.00 <sup>a</sup>	8.20 ± 3.24 <sup>a</sup>	37.56 ± 5.46 <sup>a</sup>	49.59 ± 3.87 <sup>a</sup>	56.62 ± 3.05 <sup>a</sup>	59.93 ± 2.97 <sup>a</sup>	63.73 ± 2.34 <sup>a</sup>
RG30	0.03 ± 0.00 <sup>b</sup>	12.75 ± 4.02 <sup>b</sup>	45.88 ± 3.74 <sup>b</sup>	56.90 ± 4.28 <sup>b</sup>	63.56 ± 3.81 <sup>b</sup>	65.53 ± 2.42 <sup>b</sup>	68.11 ± 3.44 <sup>b</sup>
RG40	0.04 ± 0.00 <sup>c</sup>	16.64 ± 3.69 <sup>c</sup>	54.06 ± 3.09 <sup>c</sup>	63.83 ± 2.75 <sup>c</sup>	68.41 ± 5.07 <sup>d</sup>	71.93 ± 4.26 <sup>c</sup>	73.46 ± 4.83 <sup>c</sup>

All data in the tables are expressed as mean ± standard deviation (SD). Different lowercase letters in the same column indicate significant difference ( $p < 0.05$ ).

The UV-blocking capacity was attributed to the presence of aromatic amino acids, such as tyrosine and phenylalanine, which are sensitive to UV light absorption.<sup>24</sup> In the visible range (280–800 nm), BG30 film consistently transmitted more light compared to the RG films, with transmittance values ranging from 53.29% at 300 nm to 89.10% at 800 nm. Increasing glycerol concentration significantly enhanced transmittance in the RG films. Among all treatments, the RG20 film exhibited the lowest transmittance values across all wavelengths, from 0.02% at 200 nm to 63.73% at 800 nm. This might indicate better photoprotection properties suitable for packaging applications such as oil preservation.

### 3.1.9 Thermal properties

Differential scanning calorimetry (DSC) was used to evaluate the thermal properties of the edible films, where melting temperature ( $T_m$ ) represents the temperature at which gelatin network loses its stable structure.<sup>12</sup> As shown in Figure 1a, increasing glycerol concentration resulted in a shift of the endothermic peak toward lower temperatures, from 178.46 °C (RG20) to 149.34 °C (RG40). This decrease was attributed to the plasticizing effect of glycerol, which weakened intermolecular interactions and increased the free volume within the polymer matrix, leading to a looser structure compared to films with lower glycerol content.

Consequently, less thermal energy was required to break the molecular bonds and disrupt the film network, as reflected in the decreased  $T_m$  values.<sup>7,25,32</sup> In comparison, the BG30 film exhibited a melting temperature of approximately 180 °C, which was higher than all RG films. This was attributed to the higher content of imino acids (proline and hydroxyproline) and the greater molecular weight of bovine gelatin, which enhanced hydrogen bonding and stabilized the triple helix structure within the film.<sup>15,33</sup>

### 3.1.10 FTIR

FTIR analysis was conducted to identify functional groups in gelatin-based edible films and to observe the interactions between gelatin and glycerol and structural changes in the films. The primary absorption bands are presented in Figure 1b, showing similar spectral patterns across treatments. Major peaks included amide A (3281–3285  $\text{cm}^{-1}$ , N–H stretching of  $\text{NH}_3$  groups), amide B (2930–2933  $\text{cm}^{-1}$ , asymmetric C–H stretching of aliphatic groups), amide I (1628–1633  $\text{cm}^{-1}$ , C=O stretching or H-bond coupling with  $\text{COO}^-$ ), amide II (1539–1548  $\text{cm}^{-1}$ , N–H bending and C–N stretching), and amide III (1238–1239  $\text{cm}^{-1}$ , N–H bending and C–N stretching). Variations among samples were attributed to differences in gelatin type and

glycerol concentration, affecting the secondary structures of films.<sup>15</sup>

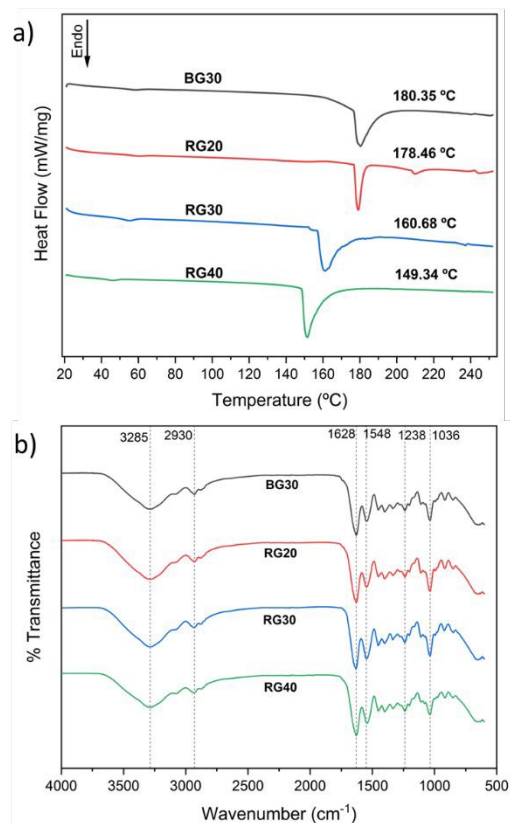


**Fig 1.** DSC thermographs (a) and FTIR spectra (b) of edible films with different glycerol concentrations.





The amide A band in BG30 ( $3281.72\text{ cm}^{-1}$ ) appeared at a slightly lower wavenumber compared to RG films ( $\sim 3285\text{ cm}^{-1}$ ), while the amide I band of BG30 film ( $1633.14\text{ cm}^{-1}$ ) was higher than RG films ( $\sim 1528\text{ cm}^{-1}$ ). These were likely due to compositional differences between bovine and rabbit bone gelatin, consistent with previous findings.<sup>34</sup> A shift of the amide B band to lower wavenumbers in RG30 film ( $2930.20\text{ cm}^{-1}$ ) and RG40 ( $2930.50\text{ cm}^{-1}$ ) compared to RG20 ( $2932.73\text{ cm}^{-1}$ ) suggested interactions between  $\text{CH}_2$  groups and  $\text{NH}_3$  moieties on protein chains.<sup>15</sup> The amide II band, related to N–H bending and C–N stretching, shifted to lower wavenumbers across films, indicating gelatin–glycerol interactions. RG20 exhibited the lowest amide II absorption, possibly due to optimal hydrogen bonding between gelatin and glycerol, resulting in reduced C–N and N–H stretching. Additionally, the absorption band at  $1036\text{ cm}^{-1}$ , corresponding to  $-\text{OH}$  groups, increased with higher glycerol concentrations, reflecting the contribution of glycerol's hydroxyl groups.<sup>35</sup> It suggested that glycerol formed new hydrogen bonds with polar groups of gelatin during film formation, disrupting intramolecular hydrogen bonding that stabilized the gelatin's triple helix structure.<sup>22,36</sup> With increasing glycerol concentration, more hydrogen bonds were formed, which in turn increased moisture content and solubility due to the hygroscopic nature of glycerol. This also enhanced flexibility, as reflected in higher elongation at break (EAB) values, while simultaneously reducing tensile strength in films with greater glycerol concentrations.

### 3.1.11 SEM

The morphology of films was investigated using SEM, as shown in Figure 2. The control film (BG30) exhibited a smooth and uniform surface, indicating effective component blending. The RG films demonstrated distinct surface textures. At lower glycerol concentration (RG20), the surface appeared rough with cracks and wrinkles, suggesting insufficient plasticization. As glycerol content increased to 30% (RG30) and 40% (RG40), the surfaces became more irregular, featuring ridges and folds. This indicated that higher glycerol content enhanced molecular mobility, although excess glycerol might have caused phase separation. Cross-sectional SEM images (Figure 3b) confirmed these findings. The BG30 film displayed a dense and compact internal structure, whereas the RG20 film appeared layered and brittle. With higher glycerol concentrations, RG films (RG30 and RG40) became more porous and less compact, indicating increased glycerol levels improved plasticity but compromised structural integrity. These changes underscored the impact of glycerol concentration on mechanical and barrier properties. Increasing glycerol content increased hydrophilic properties, disrupted polymer cohesion, and affected structural integrity, making bonds looser and more flexible.<sup>25,27</sup>

### 3.2 Oxidative stability of soybean oil in gelatin pouch

RG20 film was selected for edible oil packaging applications because it exhibited the lowest thickness ( $0.087\text{ mm}$ ), reduced moisture content ( $9.96\%$ ) and water solubility ( $31.77\%$ ), and the lowest water vapor permeability ( $0.632 \times 10^{-9}\text{ g}\cdot\text{m}^{-1}\cdot\text{Pa}^{-1}\cdot\text{s}^{-1}$ ). In

addition, it showed the highest tensile strength ( $7.34\text{ MPa}$ ), the lowest light transmittance, and the highest melting temperature ( $178.46\text{ }^\circ\text{C}$ ). Based on these combined characteristics, RG20 was chosen for comparison with LDPE in the oil packaging application. Photographs of soybean oil packaged in RG20 film and LDPE pouches are presented in Fig. 3. All soybean oil samples exhibited a yellowish color, which is attributed to the natural pigments present in the oil. Both RG20 and LDPE pouches displayed glossy and transparent surfaces, although RG20 appeared slightly more opaque than LDPE. During the 15-day storage period, no visible color changes were observed in the oil, and all pouches maintained intact seals without any signs of leakage.

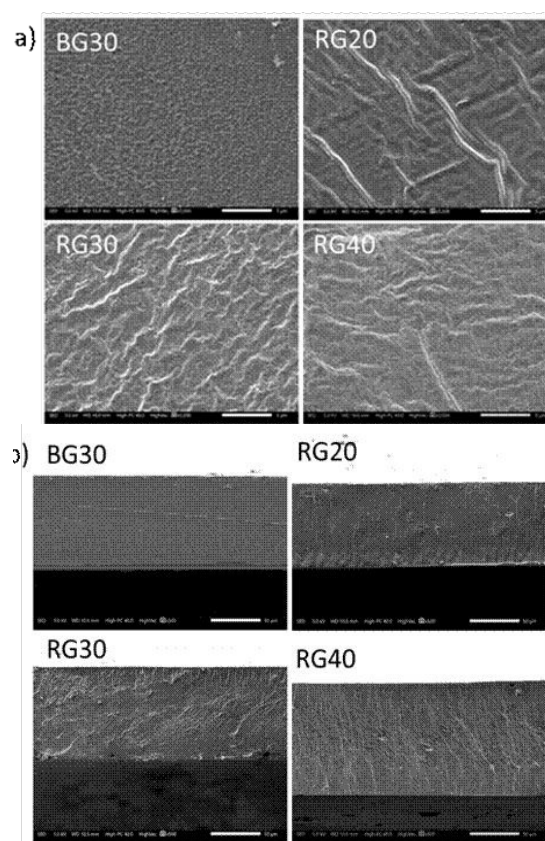


**Fig 2.** SEM micrographs of surface (a) and cross-section (b) of edible films with different glycerol concentrations.



**Fig 3.** Photographs of soybean oil packaged in RG20 film and LDPE pouches.



### 3.2.1 Peroxide value (PV)

PV measures primary oil oxidation, indicating hydroperoxide formation during early oxidation.<sup>37</sup> The findings in Figure 4a showed that the PV of soybean oil increased over a 15-day storage period in both LDPE and RG20 film packaging. On day 0, soybean oil showed low PV (1.64 meq O<sub>2</sub>/kg), indicating that the oil had low initial oxidation. At this point, the PV of the LDPE packaging exceeded the Codex Alimentarius standard (maximum 10 meq O<sub>2</sub>/kg).<sup>38</sup> In contrast, the RG20 film showed a slower increase in PV with a value of 6.57 meq O<sub>2</sub>/kg on day 9 and thus remained below the Codex standard limit, indicating a slower accumulation of primary oxidation products during the initial storage period. Consistent with previous findings, chicken skin oil stored in LDPE packaging exhibited a faster increase in peroxide value compared to oil stored in fish gelatin-based edible film packaging.<sup>39</sup> This finding may be attributed to the optical properties of the edible film in relation to ultraviolet (UV) and visible light, which warrant further investigation.

The PV value of RG20 film reached its peak (14.72 meq O<sub>2</sub>/kg) on day 15. The results demonstrated that oxidative deterioration had occurred in the soybean oil, as the peroxide value (PV) surpassed the allowable limit. The presence of residual oxygen in the headspace during the packaging process was likely responsible for this observation.<sup>40</sup> The PV reduction in LDPE packaging after day 9 likely resulted from the breakdown of hydroperoxides into secondary compounds, such as aldehydes and ketones, as detected in the anisidine value test. This matches previous findings that PV values decrease after peaking due to hydroperoxide instability.<sup>12</sup> While the RG20 film initially has lower hydroperoxide, the higher PV values at the end of storage suggested high gas and vapor permeability. This aligns with studies showing that biodegradable packaging is comparable to plastic but has lower gas migration resistance than conventional plastics.<sup>41</sup>

### 3.2.2 Anisidine value (AV)

AV indicates secondary oxidation products in later stages of lipid oxidation, such as 2-alkenals and 2,4-alkedienals, which contribute to lipid rancidity.<sup>42</sup> These compounds are formed from the degradation of hydroperoxides, which are inherently unstable. AV value is essential for evaluating the oxidative quality of oils during storage. Figure 4b showed that the AV on day 0 was minimal (1.32), indicating low initial oxidation. The AV increased significantly, particularly in RG20 film, reaching 17.08 by day 15. In contrast, the AV in LDPE packaging rose gradually, reaching 14.34 at the same time point. The greater increase in AV was observed in the RG20 film during the initial storage period. This finding suggests that while the film exhibits low WVP, its effectiveness is inferior to that of LDPE.<sup>39</sup> Consequently, this could facilitate the formation of secondary oxidation products resulting from hydroperoxide degradation.<sup>43</sup> Significant differences were observed between storage time and packaging types, showing that both factors influence oxidative degradation. Although the RG20 film exhibited a faster increase in AV during the early storage period, by days 12 and 15, the AV were not significantly different ( $p > 0.05$ ) between RG20 and LDPE packaging. This finding suggested that the edible film provided oxidative protection comparable to LDPE. Given its biodegradable nature, the edible film represented a more eco-friendly packaging alternative.<sup>44</sup> Therefore, enhancing the barrier properties of gelatin-glycerol-based packaging remains key for future research.

### 3.2.3 Free fatty acid (FFA) content

The changes in the FFA content of soybean oil during storage can be seen in Figure 4c. FFA is considered an important parameter for evaluating the hydrolytic stability of oil, as it is formed through the hydrolysis of triglycerides into free fatty acids and glycerol. An increase in FFA can be caused by enzymatic activity (e.g., lipase) or chemical reactions triggered by the presence of water and heat during storage.<sup>45</sup> During the 15-day storage period, the FFA value remained stable in LDPE and RG20 film packaging. A slight increase occurred from 1.22% (day 0) to 1.54% (day 15), indicating minimal interaction between the oil and environmental moisture that entered through the packaging. No significant differences in FFA values were observed between the two packaging types at most storage points, except on day 3, where LDPE showed a significantly higher value (1.62%) than the RG20 film (1.27%). This suggests that both packaging types offered comparable protection against hydrolytic degradation throughout storage, except for early-stage.

In contrast, peroxide and anisidine values exhibited consistent and significant differences between the two packaging types, reflecting more pronounced variation in oxidative stability. Although RG20 film was more permeable to water vapor, it did not consistently lead to higher FFA values compared to LDPE. This difference may be due to storage conditions not favoring hydrolysis reactions. These findings are consistent with previous studies reporting slow FFA accumulation during short-term storage (<1 month), unless

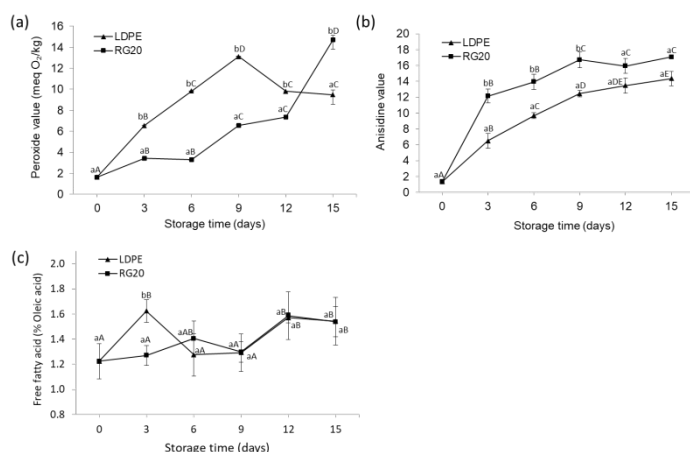


**Fig 4.** Changes in peroxide value (a), anisidine value (b) and free fatty acid (c) during soybean oil storage. Different lowercase letters indicate significant differences ( $p < 0.05$ ) among treatments within the same storage time. Different uppercase letters indicate significant differences ( $p < 0.05$ ) among storage times within the same treatment.



intensified by high lipase activity or favorable environmental conditions such as high humidity and temperature.<sup>17,45</sup>

## 4 Conclusions

The RG films were comparable to bovine gelatin film in terms of moisture content, water solubility, and water vapor permeability. Glycerol concentration significantly influenced the functional properties of RG films. Increasing glycerol from 20% to 40% elevated film thickness, moisture content, water solubility, EAB, WVP, and transmittance, while tensile strength, opacity, and thermal properties decreased. The RG film with 20% glycerol exhibited the most favorable mechanical and barrier properties. The results suggest that rabbit bone gelatin has potential as an alternative source for developing edible films. In application as soybean oil packaging, RG film showed lower primary oxidation than LDPE, although secondary oxidation occurred earlier, suggesting limitations in long-term oxidative protection. Meanwhile, free fatty acid content remained stable, indicating minimal hydrolytic degradation. These results confirm that RG films have potential as biodegradable packaging for short-term storage of soybean oil. This study represents an initial attempt to develop edible films from rabbit bone gelatin, highlighting their potential as biodegradable packaging for short-term storage of soybean oil. Future research should expand this work by incorporating additional reinforcing or active materials, as well as performing more advanced evaluations, including oxygen permeability measurements, complete DSC analysis (e.g., glass transition temperature), quantitative SEM, film integrity under real storage conditions, microbiological safety, and migration tests into oil. These directions will be essential for validating the functionality and safety of rabbit bone gelatin films in practical food packaging applications.

## Author contributions

Siti Rima Pratiwi Putri: writing – original draft, writing – review & editing, conceptualization, investigation, methodology, visualization, formal analysis, software, data curation; Dian Haryati: writing – original draft, writing – review & editing, formal analysis, software, investigation, data curation; Umar Santoso: conceptualization, writing – review & editing, project administration, supervision, validation; Andriati Ningrum: project administration, conceptualization, writing – review & editing, supervision; Ashri Nugrahini: project administration, supervision, conceptualization, writing – review & editing; Manikhanda: conceptualization, funding acquisition, writing – review & editing, project administration, supervision, resource, validation.

## Conflicts of interest

There are no conflicts to declare.

## Data availability

The data supporting this article have been included as part of the Supplementary Information.

View Article Online

DOI: 10.1039/D5FB00316D

## Acknowledgements

The research work was funded by RTA 2023 (2338/UN1/DITLIT/Dit-Lit/PT.01.00/2023) Universitas Gadjah Mada. Also, for the AE rabbit breeder group and Politeknik ATK Yogyakarta who have provided rabbit bone samples.

## References

- Liu Y, Luo D, Wang T, Hierarchical Structures of Bone and Bioinspired Bone Tissue Engineering, *Small*, 2016, **12**, 4611–32, DOI: 10.1002/smll.201600626
- Yuan K, Luo S, Zhang H, Yang X, Zhang S, Yang X, et al., Physical modification on gelation of fish gelatin by incorporating Nicandra physalodes (Linn.) Gaertn. pectin: Effect of monovalent and divalent cation ions, *Food Chem*, 2023, **405**, 134932, DOI: 10.1016/j.foodchem.2022.134932
- Hussain MA, Mishra S, Agrawal Y, Rathore D, Chokshi NP, A comparative review of biodegradable and conventional plastic packaging, *Interactions*, 2024, **245**, 126, DOI: 10.1007/s10751-024-01968-0
- Ratna, Ulfariati C, Yusmanizar, Aprilia S, Rahmiati, Munawar AA, Development of biocomposite edible film food packaging based on gelatin from chicken claw waste, *Case Stud Chem Environ Eng*, 2023, **8**, 100371, DOI: 10.1016/j.csee.2023.100371
- Rosmawati R, Sari SF, Asnani A, Embe W, Asjun A, Wibowo D, et al., Influence of Sorbitol and Glycerol on Physical and Tensile Properties of Biodegradable–Edible Film From Snakehead Gelatin and κ-Carrageenan, *Int J Food Sci*, 2025, **2025**, 7568352, DOI: 10.1155/ijfo/7568352
- Ozcan Y, Kurt A, Yildirim-Yalcin M, Toker OS, Development and structural characterisation of gelatin-based sustainable food packaging from turkey (Meleagris gallopavo) skin by-product, *Int J Food Sci Technol*, 2024, **59**, 6243–54, DOI: 10.1111/ijfs.17360
- Lau AY, Sarbon NM, Effect of glycerol concentrations on the mechanical and physical properties of chicken skin gelatin-tapioca starch composite films, *Food Res*, 2022, **6**, 428–36, DOI: 10.26656/fr.2017.6(4).546
- Lv Y, Yue H, Tan C, Liao H, Characterization of a novel biodegradable active film with rose polyphenol extract and its application in edible oil packaging, *Food Biosci*, 2025, **63**, 105784, DOI: 10.1016/j.fbio.2024.105784
- Wulandari D, Hermiyati I, Iswahyuni I, Tawarniate AZ, Production and characterization of gelatin from rabbit bone as bioplastics material by acid pre-treatment, *World Rabbit Sci*, 2022, **30**, 83–93, DOI: 10.4995/wrs.2022.16639
- Theerawitayaart W, Prodpran T, Benjakul S, Nilswan K, de la Caba K, Storage stability of fish gelatin films by molecular modification or direct incorporation of oxidized linoleic acid: Comparative studies, *Food Hydrocoll*, 2021, **113**, 106481, DOI: 10.1016/j.foodhyd.2020.106481
- Association of Official Analytical Chemist (AOAC), Official methods of analysis of the AOAC International. 21th ed., United States: AOAC; 2019.,
- Wang H, Chen X, Yang H, Wu K, Guo M, Wang X, et al., A novel gelatin composite film with melt extrusion for walnut oil





- packaging, *Food Chem*, 2025, **462**, 141021, DOI: 10.1016/j.foodchem.2024.141021
- 13 ASTM International, E96/E96M - Standard Test Methods for Water Vapor Transmission of Materials, In United States: ASTM International; 2010.,
- 14 Leite LSF, Moreira FKV, Mattoso LHC, Bras J, Electrostatic interactions regulate the physical properties of gelatin-cellulose nanocrystals nanocomposite films intended for biodegradable packaging, *Food Hydrocoll*, 2021, **113**, 106424, DOI: 10.1016/j.foodhyd.2020.106424
- 15 Hajlaoui K, Abdelhedi O, Salem A, Debeaufort F, Zouari N, Zhang Y, et al., Food-grade gelatin from camel skin: Extraction, characterisation and potential use for thin film packaging preparation, *Food Hydrocoll*, 2024, **150**, 109698, DOI: 10.1016/j.foodhyd.2023.109698
- 16 Zhang X, Ma L, Yu Y, Zhou H, Guo T, Dai H, et al., Physico-mechanical and antioxidant properties of gelatin film from rabbit skin incorporated with rosemary acid, *Food Packag Shelf Life*, 2019, **19**, 121–30, DOI: 10.1016/j.fpsl.2018.12.006
- 17 Nilsuwan K, Rajagukguk YV, Patil U, Prodpran T, Benjakul S, Fish Gelatin-Based Film Containing Maillard Reaction Products: Properties and Its Use as Bag for Packing Chicken Skin Oil, *J Renew Mater*, 2024, **12**, 1125–43, DOI: 10.32604/jrm.2024.051361
- 18 Wang S, Xia P, Wang S, Liang J, Sun Y, Yue P, et al., Packaging films formulated with gelatin and anthocyanins nanocomplexes: Physical properties, antioxidant activity and its application for olive oil protection, *Food Hydrocoll*, 2019, **96**, 617–24, DOI: 10.1016/j.foodhyd.2019.06.004
- 19 International Organization for Standardization, Determination of anisidine value - Animal and vegetable fats and oils (ISO 6885:2016), Switzerland: ISO; 2016.,
- 20 International Organization for Standardization, Animal and vegetable fats and oils - Determination of acid value and acidity (ISO 660:2020), Switzerland: ISO; 2020.,
- 21 Ma L, Yang H, Ma M, Zhang X, Zhang Y, Mechanical and structural properties of rabbit skin gelatin films, *Int J Food Prop*, 2018, **21**, 1203–18, DOI: 10.1080/10942912.2018.1476874
- 22 Chen P, Xie F, Tang F, McNally T, Unexpected Plasticization Effects on the Structure and Properties of Polyelectrolyte Complexed Chitosan/Alginate Materials, *ACS Appl Polym Mater*, 2020, **2**, 2957–66, DOI: 10.1021/acsapm.0c00433
- 23 Ng JS, Kiew PL, Lam MK, Yeoh WM, Ho MY, Preliminary evaluation of the properties and biodegradability of glycerol- and sorbitol-plasticized potato-based bioplastics, *Int J Environ Sci Technol*, 2022, **19**, 1545–54, DOI: 10.1007/s13762-021-03213-5
- 24 Abedinia A, Ariffin F, Huda N, Mohammadi Nafchi A, Preparation and characterization of a novel biocomposite based on duck feet gelatin as alternative to bovine gelatin, *Int J Biol Macromol*, 2018, **109**, 855–62, DOI: 10.1016/j.ijbiomac.2017.11.051
- 25 Tarique J, Sapuan SM, Khalina A, Effect of glycerol plasticizer loading on the physical, mechanical, thermal, and barrier properties of arrowroot (*Maranta arundinacea*) starch biopolymers, *Sci Rep*, 2021, **11**, 13900, DOI: 10.1038/s41598-021-93094-y
- 26 Hazrol MD, Sapuan SM, Zainudin ES, Zuhri MYM, Abdul Wahab NI, Corn Starch (*Zea mays*) Biopolymer Plastic Reaction in Combination with Sorbitol and Glycerol, *Polymers*, 2021, **13**, 242, DOI: 10.3390/polym13020242
- 27 Galus S, Gaouditz M, Kowalska H, Debeaufort F, Effects of Candelilla and Carnuba Wax Incorporation on the Functional Properties of Edible Sodium Caseinate Films, *Int J Mol Sci*, 2020, **21**, 9349, DOI: 10.3390/ijms21249349 DOI: 10.1039/D5FB00316D
- 28 Mosleh Y, de Zeeuw W, Nijemeisland M, Bijleveld JC, van Duin P, Poullis JA, The Structure–Property Correlations in Dry Gelatin Adhesive Films, *Adv Eng Mater*, 2021, **23**, 2000716, DOI: 10.1002/adem.202000716
- 29 Kusmono, Wildan MW, Lubis FI, Fabrication and Characterization of Chitosan/Cellulose Nanocrystal/Glycerol Bio-Composite Films, *Polymers*, 2021, **13**, 1096, DOI: 10.3390/polym13071096
- 30 Said NS, Sarbon NM, Physical and Mechanical Characteristics of Gelatin-Based Films as a Potential Food Packaging Material: A Review, *Membranes*, 2022, **12**, 442, DOI: 10.3390/membranes12050442
- 31 Hamdi M, Nasri R, Li S, Nasri M, Bioactive composite films with chitosan and carotenoproteins extract from blue crab shells: Biological potential and structural, thermal, and mechanical characterization, *Food Hydrocoll*, 2019, **89**, 802–12, DOI: 10.1016/j.foodhyd.2018.11.062
- 32 Chen Y, Wang J, Xu L, Nie Y, Ye Y, Qian J, et al., Effects of Different Plasticizers on the Structure, Physical Properties and Film Forming Performance of Curdlan Edible Films, *Foods*, 2024, **13**, 3930, DOI: 10.3390/foods13233930
- 33 Suderman N, Isa MIN, Sarbon NM, Characterization on the mechanical and physical properties of chicken skin gelatin films in comparison to mammalian gelatin films, *IOP Conf Ser Mater Sci Eng*, 2018, **440**, 012033, DOI: 10.1088/1757-899X/440/1/012033
- 34 Jovanović M, Tomić N, Cvijić S, Stojanović D, Ibrić S, Uskoković P, Mucoadhesive Gelatin Buccal Films with Propranolol Hydrochloride: Evaluation of Mechanical, Mucoadhesive, and Biopharmaceutical Properties, *Pharmaceutics*, 2021, **13**, 273, DOI: 10.3390/pharmaceutics13020273
- 35 Ooi KS, Haszman S, Wong YN, Soidin E, Hesham N, Mior MAA, et al., Physicochemical Characterization of Bilayer Hybrid Nanocellulose-Collagen as a Potential Wound Dressing, *Materials*, 2020, **13**, 4352, DOI: 10.3390/ma13194352
- 36 Smith DR, Escobar AP, Andris MN, Boardman BM, Peters GM, Understanding the Molecular-Level Interactions of Glucosamine-Glycerol Assemblies: A Model System for Chitosan Plasticization, *ACS Omega*, 2021, **6**, 25227–34, DOI: 10.1021/acsomega.1c03016
- 37 Singh PK, Chopra R, Garg M, Comparative study on the use of rosemary bioactive for enhancing the oxidative stability of blended perilla seed oil: A multivariant kinetic approach, *Food Chem Adv*, 2023, **3**, 100447, DOI: 10.1016/j.focha.2023.100447
- 38 Food and Agriculture Organization, Standard for Named Vegetable Oils (CODEX STAN 210-1999), Rome: FAO; 2024.,
- 39 Nilsuwan K, Benjakul S, Prodpran T, de la Caba K, Fish gelatin monolayer and bilayer films incorporated with epigallocatechin gallate: Properties and their use as pouches for storage of chicken skin oil, *Food Hydrocoll*, 2019, **89**, 783–91, DOI: 10.1016/j.foodhyd.2018.11.056
- 40 Ashrafi A, Babapour H, Johari S, Alimohammadi F, Teymori F, Nafchi AM, et al., Application of Poultry Gelatin to Enhance the Physicochemical, Mechanical, and Rheological Properties of Fish Gelatin as Alternative Mammalian Gelatin Films for Food Packaging, *Foods*, 2023, **12**, 670, DOI: 10.3390/foods12030670
- 41 Sánchez-Gutiérrez M, Bascón-Villegas I, Espinosa E, Carrasco E, Pérez-Rodríguez F, Rodríguez A, Cellulose Nanofibers from Olive Tree Pruning as Food Packaging Additive of a Biodegradable Film, *Foods*, 2021, **10**, 1584, DOI: 10.3390/foods10071584



- 42 Skiera C, Steliopoulos P, Kuballa T, Holzgrabe U, Diehl B, 1H NMR approach as an alternative to the classical p-anisidine value method, *Eur Food Res Technol*, 2012, **235**, 1101–5, DOI: 10.1007/s00217-012-1841-5
- 43 Nilsuwan K, Guerrero P, Caba K de la, Benjakul S, Prodpran T, Properties of fish gelatin films containing epigallocatechin gallate fabricated by thermo-compression molding, *Food Hydrocoll*, 2019, **97**, 105236, DOI: 10.1016/j.foodhyd.2019.105236
- 44 Lu Y, Luo Q, Chu Y, Tao N, Deng S, Wang L, et al., Application of Gelatin in Food Packaging: A Review, *Polymers*, 2022, **14**, 436, DOI: 10.3390/polym14030436
- 45 Emebu S, Osaikhuiwuomwan O, Mankonen A, Udoeye C, Okieimen C, Janáčová D, Influence of moisture content, temperature, and time on free fatty acid in stored crude palm oil, *Sci Rep*, 2022, **12**, 9846, DOI: 10.1038/s41598-022-13998-1

View Article Online  
DOI: 10.1039/D5FB00316D





**Data Availability Statement**

The data supporting this article have been included as part of the Supplementary Information.

